

Impaired Lysosomal Function Underlies Monoclonal Light Chain–Associated Renal Fanconi Syndrome

Alessandro Luciani,* Christophe Sirac,^{†‡} Sara Terryn,[§] Vincent Javaugue,^{†||} Jenny Ann Prange,* Sébastien Bender,^{†||} Amélie Bonaud,[†] Michel Cogné,[†] Pierre Aucouturier,^{||} Pierre Ronco,^{**††‡‡} Frank Bridoux,^{†||} and Olivier Devuyst*[§]

*Institute of Physiology, Zurich Center for Integrative Human Physiology, University of Zurich, Zurich, Switzerland; [†]Department of Immunology, National Center for Scientific Research, Joint Research Unit 7276, University of Limoges, Limoges, France; [‡]National Reference Center for Amyloidosis and other Monoclonal Immunoglobulin Deposition Diseases, University Hospital of Limoges, Poitiers, France; [§]Division of Nephrology, UCL Medical School, Brussels, Belgium; ^{||}Department of Nephrology, University Hospital, Poitiers University, Poitiers, France; ^{||}Department of Immunology, National Institute of Health and Medical Research Unit 938, Saint Antoine Hospital, Pierre et Marie Curie University, Paris, France; ^{**}Department of Nephrology and Dialysis, Tenon Hospital, Paris, France; ^{††}Department of Immunology, National Institute of Health and Medical Research Unit 938, Saint Antoine Hospital, Pierre et Marie Curie University, Department of Nephrology and Dialysis, Tenon Hospital, Paris, France; ^{‡‡}Sorbonne Universités, UPMC University of Paris, Paris, France

ABSTRACT

Monoclonal gammopathies are frequently complicated by kidney lesions that increase the disease morbidity and mortality. In particular, abnormal Ig free light chains (LCs) may accumulate within epithelial cells, causing proximal tubule (PT) dysfunction and renal Fanconi syndrome (RFS). To investigate the mechanisms linking LC accumulation and PT dysfunction, we used transgenic mice overexpressing human control or RFS-associated κ LCs (RFS- κ LCs) and primary cultures of mouse PT cells exposed to low doses of corresponding human κ LCs (25 μ g/ml). Before the onset of renal failure, mice overexpressing RFS- κ LCs showed PT dysfunction related to loss of apical transporters and receptors and increased PT cell proliferation rates associated with lysosomal accumulation of κ LCs. Exposure of PT cells to RFS- κ LCs resulted in κ LC accumulation within enlarged and dysfunctional lysosomes, alteration of cellular dynamics, defective proteolysis and hydrolase maturation, and impaired lysosomal acidification. These changes were specific to the RFS- κ LC variable (V) sequence, because they did not occur with control LCs or the same RFS- κ LC carrying a single substitution (Ala30→Ser) in the V domain. The lysosomal alterations induced by RFS- κ LCs were reflected in increased cell proliferation, decreased apical expression of endocytic receptors, and defective endocytosis. These results reveal that specific κ LCs accumulate within lysosomes, altering lysosome dynamics and proteolytic function through defective acidification, thereby causing dedifferentiation and loss of reabsorptive capacity of PT cells. The characterization of these early events, which are similar to those encountered in congenital lysosomal disorders, provides a basis for the reported differential LC toxicity and new perspectives on LC-induced RFS.

J Am Soc Nephrol 27: ●●–●●●, 2016. doi: 10.1681/ASN.2015050581

Received May 27, 2015. Accepted October 5, 2015.

A.L. and C.S. contributed equally to this work.

Published online ahead of print. Publication date available at www.jasn.org.

Correspondence: Dr. Frank Bridoux, Department of Nephrology

and Kidney Transplantation, University Hospital La Milétrie, 86021 Poitiers, France, or Dr. Olivier Devuyst, Institute of Physiology, University of Zurich, Winterthurerstrasse 190, CH-8057 Zurich, Switzerland. Email: f.bridoux@chu-poitiers.fr or olivier.devuyst@uzh.ch

Copyright © 2016 by the American Society of Nephrology

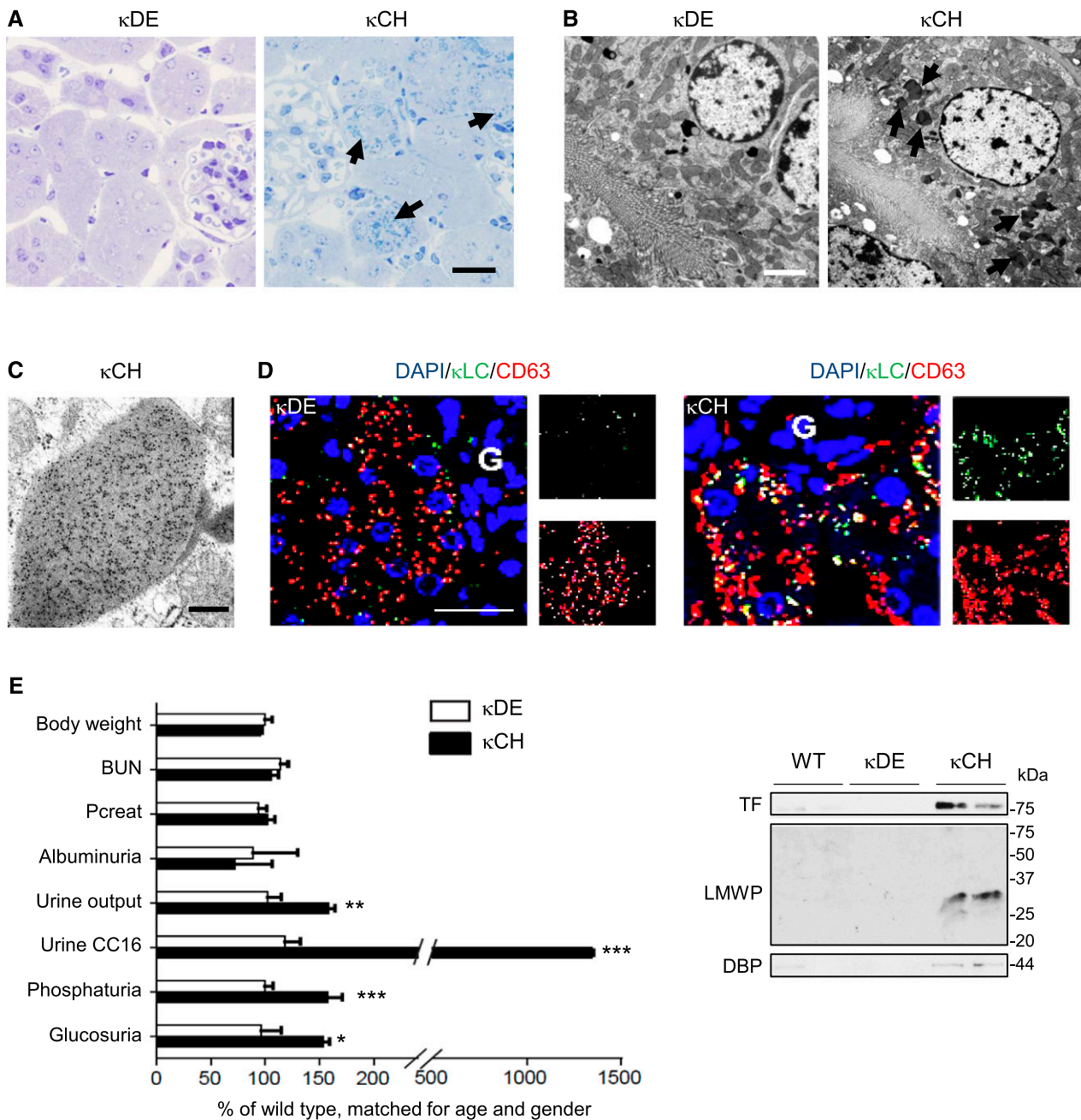


Figure 1. Specific κ LCs accumulate in lysosomes of mPTCs in mouse kidney. (A) Semithin, toluidine blue–stained kidney sections showing numerous crystalline inclusions in proximal tubule cells of κ CH mice (arrows) compared with normal appearance in κ DE mice. Scale bar, 50 μ m. (B) Electron microscopy revealing crystalline and osmiophilic inclusions (arrows) surrounded by a single membrane within proximal tubular cells of κ CH versus κ DE kidneys. Scale bar, 2 μ m. (C) Immunogold labeling shows strongly positive crystals labeled with anti- κ LC in κ CH kidneys. Scale bar, 0.1 μ m. (D) Confocal microscopy illustrating colocalization of κ LC-positive dots (green) with CD63-positive vesicles (red) in proximal tubule cells of κ DE and κ CH kidneys. Nuclei counterstained with DAPI (blue). G, glomerulus. Scale bar, 30 μ m. (E) Clinical and biologic parameters obtained from κ DE and κ CH mice compared with WT controls matched for age and gender. The κ CH mice show polyuria, glucosuria, phosphaturia, and increased urinary excretion of Clara cell protein 16 (CC16) compared with WT controls and κ DE mice. Body weight, BUN, and plasma creatinine (Pcreat) levels are similar. * $P < 0.05$ (κ CH compared with WT and κ DE; $n = 7$ mice per group); ** $P < 0.01$ (κ CH compared with WT and κ DE; $n = 7$ mice per group); *** $P < 0.001$ (κ CH compared with WT and κ DE; $n = 7$ mice per group). (E, Inset) Representative immunoblots for low molecular weight protein (LMWP), vitamin D–binding protein (DBP), and transferrin (TF) in urine samples from WT, κ CH, and κ DE mice. Loading was normalized to urinary creatinine concentration. DAPI, 4', 6'-diamidino-2-phenylindole.

Table 1. Body weight, urine, and blood parameters in WT and κ LC transgenic mice

Parameter	WT	κ CH	κ DE
Body weight (g)	27.8±0.5	26.5±0.5	27.9±1.8
U volume (μ l/24 h)	1361±92	2024±153 ^a	1384±176
U albumin (μ M/mg creatinine per deciliter)	1073±143	776±266	957±395
U CC16 (μ g/g creatinine)	11±1.5	148±13.3 ^b	20±7.8
U calcium (mg/g creatinine)	64±4	53±4	97±15
U phosphate (mg/g creatinine)	87±7	133±7.5 ^b	84±16
U glucose (mg/g)	1.4±0.2	2.2±0.3 ^c	1.4±0.1
U creatinine (mg/dl)	62±4	57±6	61±9
BUN (mg/dl)	21±1.2	22±1.6	24±1.7
P creatinine (mg/dl)	0.094±0.01	0.096±0.01	0.09±0.01

Seven mice per group. U, urine; CC16, Clara cell protein; P, plasma.

^a $P < 0.01$ versus the WT and κ DE.

^b $P < 0.001$ versus the WT and κ DE.

^c $P < 0.05$ versus the WT and κ DE.

The kidney is the most commonly involved organ in monoclonal gammopathies, causing a range of complications that increase the morbidity and mortality of the disease.^{1,2} In normal conditions, the kidney is essential for the clearance of free light chains (LCs) produced by plasma cells.³ The polyclonal LCs are filtered by the glomerulus and like other low molecular weight (LMW) proteins, reabsorbed in proximal tubule (PT) cells by receptor-mediated endocytosis. The latter involves two multiligand receptors, megalin and cubilin, that are expressed in the apical membrane of PT cells.⁴ After binding and internalization into coated vesicles, LCs are delivered to the endolysosomal compartment for degradation, so that they are virtually absent from final urine.⁵

Plasma cell disorders are often characterized by an overproduction of monoclonal LCs with abnormal physicochemical characteristics. These LCs can overwhelm the endocytic capacity of PT cells, being then lost in urine,⁶ whereas their intracellular accumulation leads to tubulointerstitial inflammation and fibrosis through different pathways that include oxidative stress, activation of NF- κ B, and release of inflammatory mediators.^{3,7} In high-mass myeloma, massive quantities of LCs in distal tubular segments may trigger the formation of casts that obstruct the lumen, also leading to tubulointerstitial fibrosis.⁶ Alternatively, monoclonal LCs may cause renal Fanconi syndrome (RFS), a general dysfunction of PT cells leading to the urinary leak of LMW proteins, phosphate, uric acid, glucose, and amino acids often associated with osteomalacia and progressive renal failure. In contrast with cast nephropathy, RFS is mostly observed in patients with smoldering myeloma or isolated monoclonal gammopathy.^{8,9} Monoclonal gammopathy is a main cause of RFS in adults >50 years of age.¹⁰ PT dysfunction and RFS may also result from congenital disorders, such as Dent disease and cystinosis, with defective receptor-mediated endocytosis as a common feature.^{11–13}

There is a remarkable heterogeneity in the capacity of free LCs to induce renal tubular damage. Only some LCs are nephrotoxic, and when they are, the pattern of tubular injuries is heterogeneous.¹⁴ If a broad range of LCs can induce cellular

stress and inflammation when administered at high dose *in vitro* or *ex vivo* in experimental models,^{15–17} only limited sequence peculiarities of the variable (V) region can lead to specific development of cast nephropathy or RFS in humans. Most LCs involved in RFS belong to the V κ 1 subgroup, derive from two germ-line genes (V κ 1–33 and V κ 1–39), and present mutations in the V domain conferring a resistance to proteolysis,¹⁸ leading to the formation of intracytoplasmic crystals in mice injected with the corresponding clones.¹⁹ Because of the limitations of cellular and animal models,²⁰ the short-term exposure to LCs of perfused tubule systems, and the systemic repercussions of LCs-expressing

tumor grafts,^{15–19} the molecular mechanisms sustaining the specific toxicity of κ LCs are poorly understood. In particular, whether the activity of the endolysosomal system is modified and how such changes affect tubular epithelial differentiation during the course of LCs-associated RFS remain unknown.

The aim of this study was to analyze the specific effect of monoclonal human κ LCs responsible for RFS (RFS- κ LCs) or other confirmed renal manifestations before the onset of renal failure. We investigated transgenic mice expressing similar levels of human κ LCs from a patient with RFS (κ CH mice)²¹ or a patient with biopsy-proven renal AL amyloidosis but without RFS and kidney damage (κ DE mice). We also exposed primary cultured cells isolated from PT segments of mouse kidney to low doses of human κ LCs. These cells, which keep their differentiation and polarized transport processes, provide a particularly well suited model to investigate receptor-mediated endocytosis of apical ligands and their lysosomal processing.^{13,22,23} We show that specific RFS- κ LCs accumulate within lysosomes of PT cells, causing marked alterations in cell dynamics and lysosomal function. In turn, these alterations promote dedifferentiation of the cells and defective receptor-mediated endocytosis, sustaining the loss of reabsorptive capacity of the kidney tubule.

RESULTS

Accumulation of Specific RFS- κ LCs Induces PT Dysfunction in Mouse

We first analyzed the mechanism of κ LCs toxicity *in vivo* using κ CH and κ DE mice. Intracellular rhomboid crystals were evidenced in κ CH kidneys (Figure 1A), with no other structural damage. The κ LCs inclusions were exclusively detected in κ CH kidneys, unrelated to the amount of free κ LCs in the urine (Supplemental Figure 1A). They were located within multivesicular body-like structures from the late endolysosomal compartment (Figure 1, B and C), which was confirmed by colocalization in CD63-positive vesicles (Figure 1D).

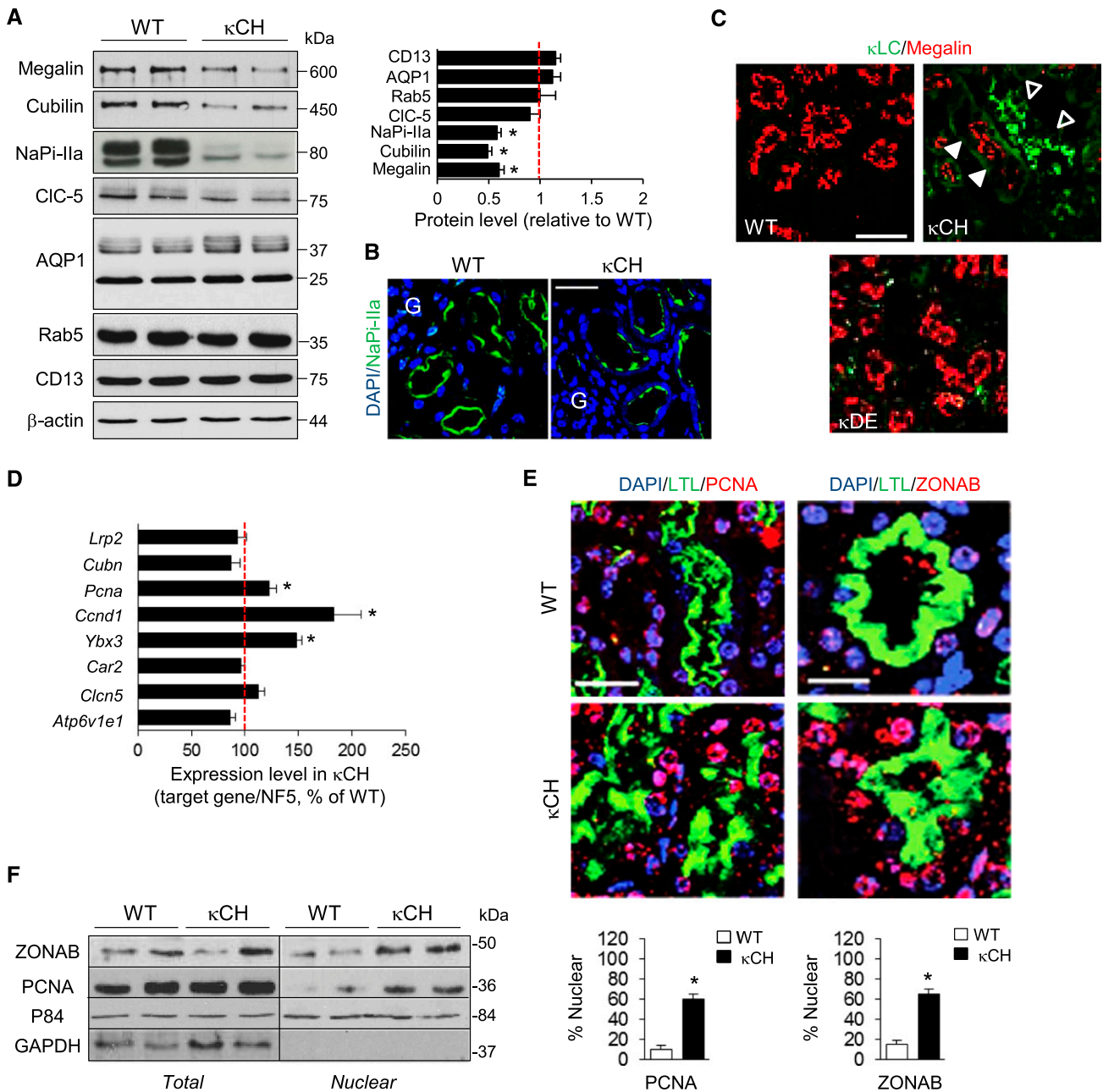


Figure 2. Dedifferentiation and proliferation in mPTCs of κ CH kidneys. (A) Representative immunoblots and densitometry analyses for megalin, cubilin, NaPi-IIa, CIC-5, AQP1, Rab5a, and aminopeptidase (CD13) in κ CH and WT kidneys (20 μ g total protein per lane). * $P < 0.05$ versus WT (taken as 100%; $n = 5$ mice per group). (B) Immunofluorescence for NaPi-IIa in WT and κ CH kidneys. Nuclei were counterstained with DAPI (blue). G, glomerulus. Scale bar, 50 μ m. (C) Double immunostaining for megalin (red) and κ LCs (green) in WT, κ DE, and κ CH kidneys. The accumulation of κ LCs in some tubule profiles is reflected by a decreased immunoreactivity for megalin in κ CH kidneys. Scale bar, 50 μ m. (D) Quantitative RT-PCR to measure the mRNA expression of PT (*Lrp2*, *Cubn*, *Car2*, *Cln5*, and *Atp6v1e1*) and proliferation (*Pcna*, *Ccnd1*, and *Ybx3*) genes in κ CH and WT whole kidneys. The normalization factor was calculated from five different housekeeping genes. * $P < 0.05$ versus WT ($n = 6$ mice per group). (E, top and middle panels) Double immunofluorescence for (E, left panel) PCNA (red) or (E, right panel) ZONAB (red) and the PT marker Lotus Tetragonolobus Lectin (LTL; green) in WT and κ CH kidneys. Nuclei were counterstained with DAPI (blue). Scale bar, 20 μ m. (E, bottom panel) Quantification of LTL-positive mPTCs presenting nuclear PCNA or ZONAB immunoreactivity (%). * $P < 0.05$ κ CH versus WT kidneys ($n = 100$ LTL-positive cells). (F) Representative immunoblots for ZONAB and PCNA in total and nuclear fractions (P84 enriched and GAPDH depleted) extracted from WT and κ CH kidneys ($n = 5$ mice per group). DAPI, 4', 6'-diamidino-2-phenylindole; GAPDH, glyceraldehyde 3-phosphate dehydrogenase.

Table 2. Characteristics of the human LCs used in the study

LC	Kidney Disease	Isotype	V (L) Domain	Mutations of Interest ^a	Crystal Formation ^b	pI (V Domain)	Charge (pH 7/pH 5)	Aggregation Score (V Domain) ^c	Reference
CH	RFS	κ	V κ 1–39	A30; I94	Yes	8.45	1.9/3.2	486.69	1,6
DU	RFS	κ	V κ 1–5	V31	Yes	5.17	–1.1/0.4	897.65	—
CHm	—	κ	V κ 1–39	A30→S	No	8.45	1.9/3.2	229.12	6
DE	AL amyloidosis	κ	V κ 1–33	F52	No	5.36	–1.1/1.0	332.77	—
RO	Cast nephropathy	κ	V κ 2–28	A51;Y52	No	7.09	0.1/3.0	595.71	—

V(L), variable domain; pI, isoelectric point; DU, RFS-kLC; —, not causing kidney disease; AL, amyloid light chain; CDR, complementary determining region; TANGO, algorithm used to predict the aggregating regions in the V(L) domain.

^aPolar to hydrophobic residue substitution in solvent-exposed loops (CDR).

^bCrystal formation was documented by electron microscopy study of the kidney biopsy.

^cAggregation score obtained using the TANGO algorithm.

To test whether lysosomal accumulation of κ LCs induces PT dysfunction, we performed metabolic cage studies in age- and sex-matched wild-type (WT) versus κ DE and κ CH mice (Figure 1E, Table 1). Compared with WT and κ DE, κ CH mice showed classic features of RFS, such as polyuria, glycosuria, phosphaturia, and LMW proteinuria, including megalin (Clara cell protein and vitamin D-binding protein) and cubilin (transferrin) ligands, without changes in plasma creatinine and BUN levels.

RFS- κ LCs Decrease Apical Receptors and Transporters and Increase Cell Proliferation

We next investigated the mechanisms of PT dysfunction secondary to lysosomal accumulation of RFS- κ LCs. There was an approximately 40%–50% decrease of megalin/cubilin protein levels and NaPi-IIa in κ CH kidneys versus WT littermates, whereas other PT cell components, such as the water channel AQP1, the endocytic catalyst Rab5a, the endosomal chloride-proton exchanger ClC-5, and the brush border component CD13 (aminopeptidase N), were unaffected (Figure 2, A and B). None of these changes was observed in κ DE kidneys (Supplemental Figure 1B). The cell-specific effect of κ LCs was shown by a decreased apical expression of megalin restricted to κ LCs-accumulating PT cells in κ CH kidneys, contrasting with preserved expression in κ DE kidneys (Figure 2C). The decreased expression of endocytic receptors in κ CH kidneys was unrelated to decreased mRNA levels (Figure 2D), suggesting a role for defective endomembrane trafficking.¹²

A defective expression of apical receptors may reflect imbalance between differentiation and proliferation.^{13,24} Analyses of κ CH kidneys revealed a marked increase in the expression of proliferative markers (proliferating cell nuclear antigen *Pcna*, *Ccnd1*, and *Ybx3/ZONAB*) (Figure 2D) associated with nuclear translocation of PCNA and ZONAB (Figure 2, E and F). Conversely, neither the expression nor the nuclear location of PCNA or ZONAB was consistently altered in κ DE kidneys (Supplemental Figure 1, C and D).

RFS- κ LCs Accumulate in Lysosomes through Improper Degradation

To gain mechanistic insights into the accumulation of RFS- κ LCs, we used the well established system of primary cultures of mouse proximal tubule cells (mPTCs) that deliver apical ligands to either

the recycling compartment or lysosomes for degradation.^{13,22} The mPTCs were exposed to low doses (25 μ g/ml) of human κ LCs associated with RFS (κ CH or κ DU), cast nephropathy (κ RO), AL amyloidosis without RFS (κ DE), or a mutant version of κ CH (κ CHm) (Supplemental Figure 2, A and B, Table 2). κ CHm was obtained by directed mutagenesis of κ CH, replacing the hydrophobic Ala at position 30 in V domain by the polar Ser that prevents crystal formation in PT cells.¹⁹ The Ala30→Ser mutation does not modify the isoelectric point or global structure of the V κ domain but has a substantial effect on the predictive aggregation score (Supplemental Figure 2B, Table 2). Because RFS- κ LCs accumulation in PT cells could be associated with a peculiar resistance of V κ domain to proteolysis,²⁵ we performed *in vitro* cathepsin-B digestion of the V κ 1 LCs. Only κ DE showed complete degradation at 3 hours, whereas all other κ LCs displayed a 12-kD fragment corresponding to the V domain resistant to digestion (Supplemental Figure 2C). Thus, the Ala30→Ser mutation in κ CHm did not affect cathepsin-B resistance.

Exposure of mPTCs for 60 minutes to 25 μ g/ml κ LCs followed by chase \leq 24 hours resulted in a rapid delivery of κ LCs to intracellular vesicles as scored by real-time confocal microscopy (Figure 3A). Internalization of κ LCs was blocked when cells were preincubated with methyl- β -cyclodextrin, which inhibits clathrin-mediated endocytosis, or filipin, a specific inhibitor of lipid raft- or caveolae-dependent endocytosis (Supplemental Figure 3), confirming that endocytosis dictates the intracellular trafficking of κ LCs in this system like *in vivo*.²⁶

After internalized, control κ LCs (κ RO, κ DE, and κ CHm) showed a diffuse distribution throughout the cytoplasm, which faded over time (Figure 3A). In contrast, incubation with either κ CH or κ DU led to a sustained κ LC staining pattern, with strong, perinuclear clustering (Figure 3A). The latter overlapped with CD63-positive lysosomes (Figure 3B, left panel) (data not shown for κ DU), showing the prolonged retention (or defective processing) of RFS- κ LCs within lysosomes. The marked increase in CD63-positive vesicles containing κ CHm and κ RO in the presence of Bafilomycin-A1, an inhibitor of lysosomal acidification, further confirmed that the reduction of signal over time was caused by lysosomal degradation (Figure 3B, right panel). Taken together, these results showed that RFS- κ LCs accumulate in lysosomes through improper degradation independently of their *in vitro* resistance to proteolysis.

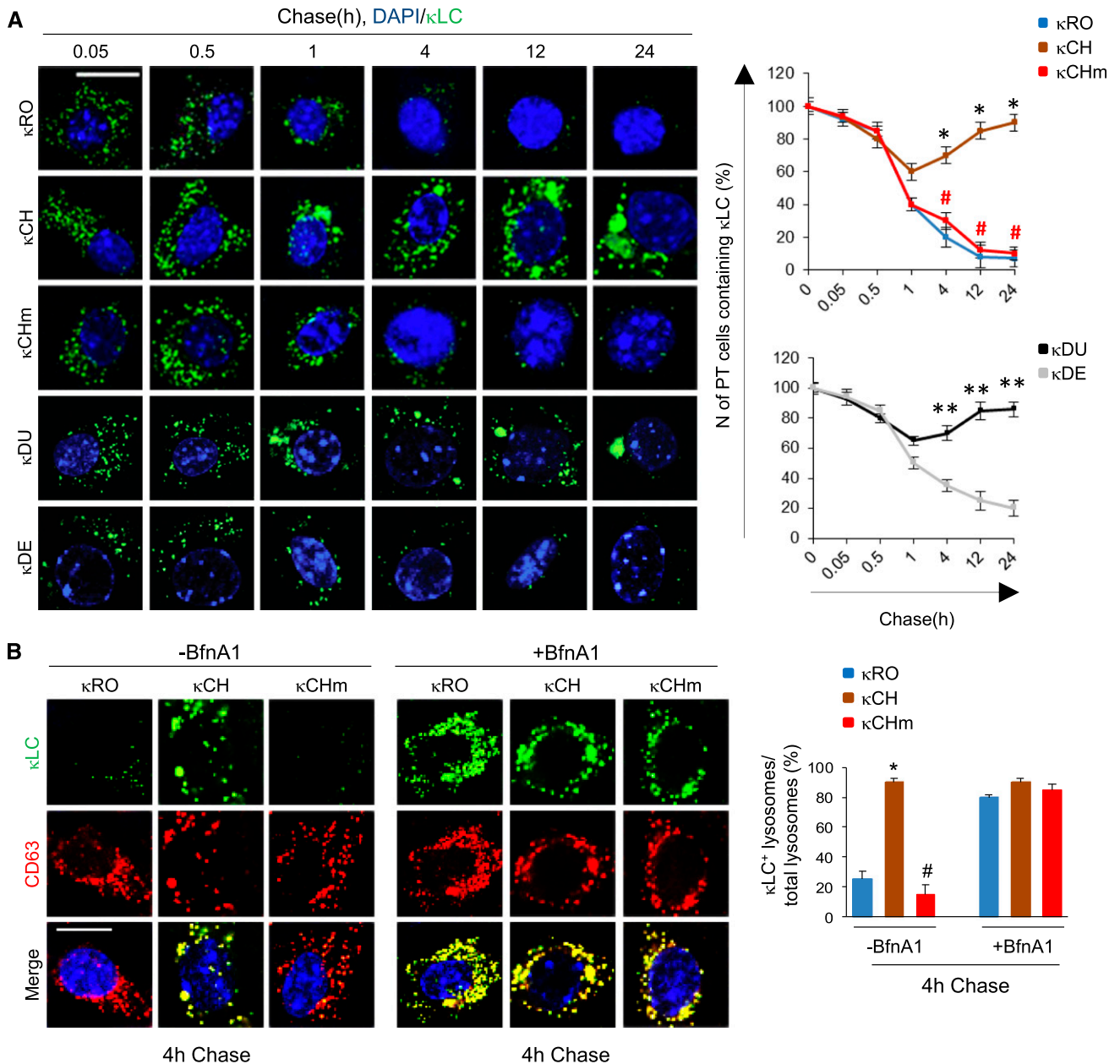


Figure 3. RFS-κLCs are retained within lysosomes. Primary mPTCs were initially kept for 4 hours in serum-free culture medium, incubated with 25 μg/ml human κLCs for 1 hour at 4°C, and then, chased in κLCs-free culture medium for the indicated times at 37°C. Where drug treatment was performed, cells were incubated with Bafilomycin-A1 (+BfnA1; 250 nM) during the pulse and chase (total of 6 hours). (A) The cells were fixed and stained with an anti-κLC antibody. Nuclei were counterstained with DAPI (blue). Scale bar, 10 μm. (A, right panel) Quantification of cells containing κLCs. **P*<0.05 κCH versus κRO (*n*=200 cells per group); #*P*<0.01 κCHm versus κCH (*n*=200 cells per group); ***P*<0.01 κDU versus κDE (*n*=200 cells per group). (B) Double immunofluorescence staining for κLCs (green) and CD63 (red). Nuclei were counterstained with DAPI (blue). Scale bar, 10 μm. (B, right panel) Quantitative measurement of number of lysosomes containing κLCs (percentage of total lysosomes). **P*<0.05 κCH versus κRO (*n*=200 cells per group); #*P*<0.01 κCHm versus κCH (*n*=200 cells per condition). DAPI, 4', 6'-diamidino-2-phenylindole.

RFS-κLCs Specifically Alter Lysosomal Dynamics

In light of the endomembrane reorganization, we next evaluated a potential effect of κLCs on lysosome dynamics by monitoring the lysosome-associated membrane protein type 1 (LAMP1), which typically transits through the

endolysosomal pathway. Confocal microscopy revealed that LAMP1-positive lysosomes were dispersed throughout the cytosol in mPTCs exposed to κRO, κCHm, or κDE, whereas they aggregated in the perinuclear region in cells exposed to RFS-κLCs (κCH or κDU) (Figure 4, A and F). The perinuclear

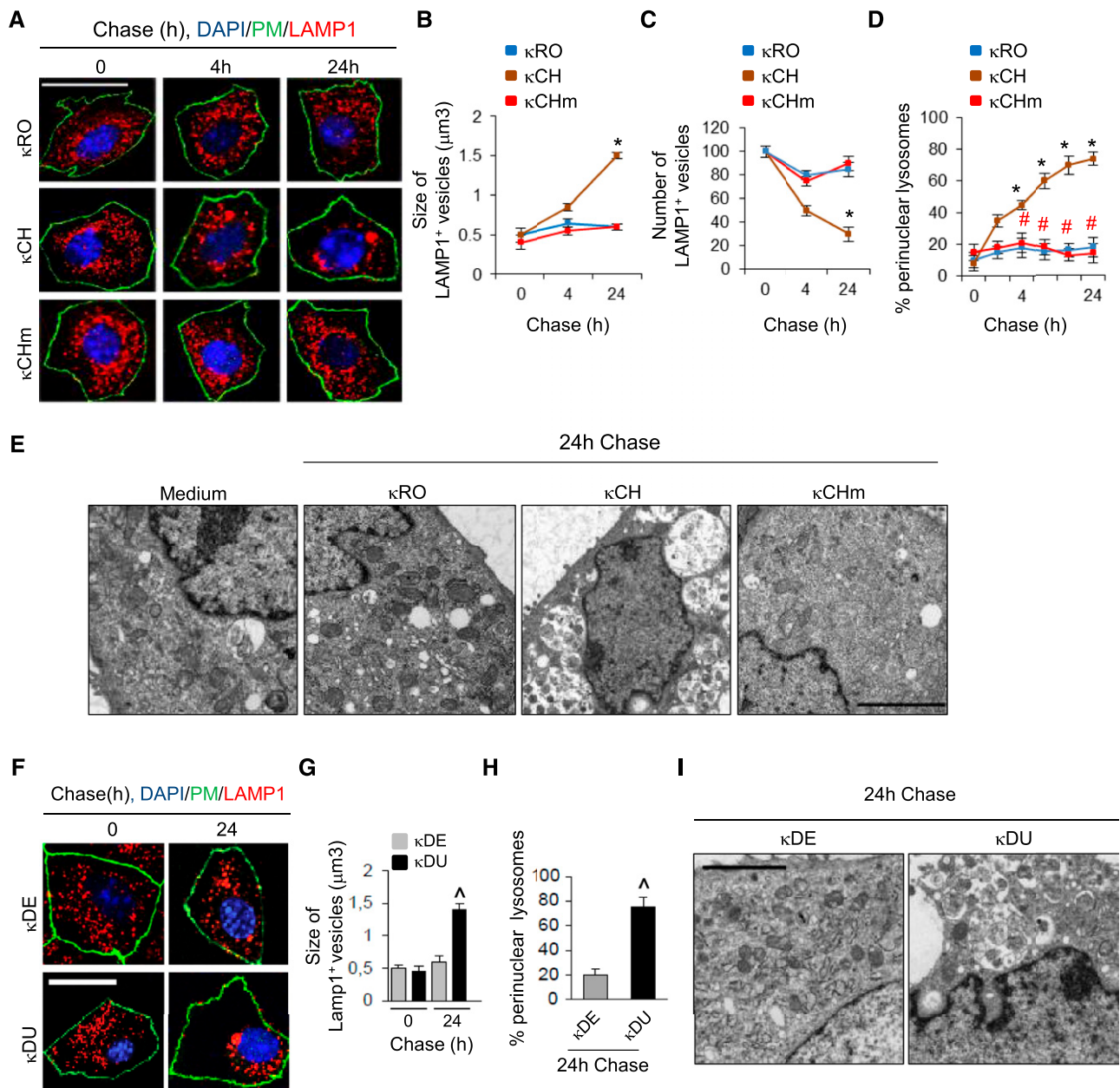


Figure 4. RFS- κ LCs alter lysosomal dynamics. Primary mPTCs were initially kept for 4 hours in serum-free medium, incubated with 25 μ g/ml human κ LCs for 1 hour at 4°C, and then, chased in κ LCs-free culture medium for the indicated times at 37°C. (A and F) Double immunofluorescence for LAMP1 (red) and plasma membrane marker (PM; green) in mPTCs exposed to κ LCs for \leq 24 hours. Nuclei were counterstained with DAPI (blue). Scale bar, 10 μ m. The adjacent panels show quantification of changes in (B and G) vesicle size, (C) number, and (D and H) lysosome position. * P <0.05 κ CH versus κ RO (n =200 cells per condition); # P <0.01 κ CHm versus κ CH (n =200 cells per condition) \wedge P <0.05 κ DU versus κ DE. (E and I) Electron microscopy of mPTCs exposed to either κ CH or κ DU shows accumulation of single-membrane structures containing cytosolic constituents. No crystalline inclusion was observed. Scale bar, 0.5 μ m. DAPI, 4', 6'-diamidino-2-phenylindole.

clustering of LAMP1-positive vesicles in cells exposed to RFS- κ LCs as well as their increase in size and reduction in number were confirmed by automated confocal analysis (Figure 4, B–D, G, and H). Electron microscopy studies confirmed the accumulation of abnormal, single-membrane structures engulfed by intact or partly degraded cytosolic constituents in

mPTCs exposed to κ CH or κ DU compared with cells exposed to κ RO, κ CHm, or κ DE (Figure 4, E and I). This accumulation was reflected by a 2-fold increase in LAMP1 protein, despite unchanged mRNA levels (data not shown).

The major effect of RFS- κ LCs on lysosomal dynamics did not result from abnormal trafficking through the endocytic

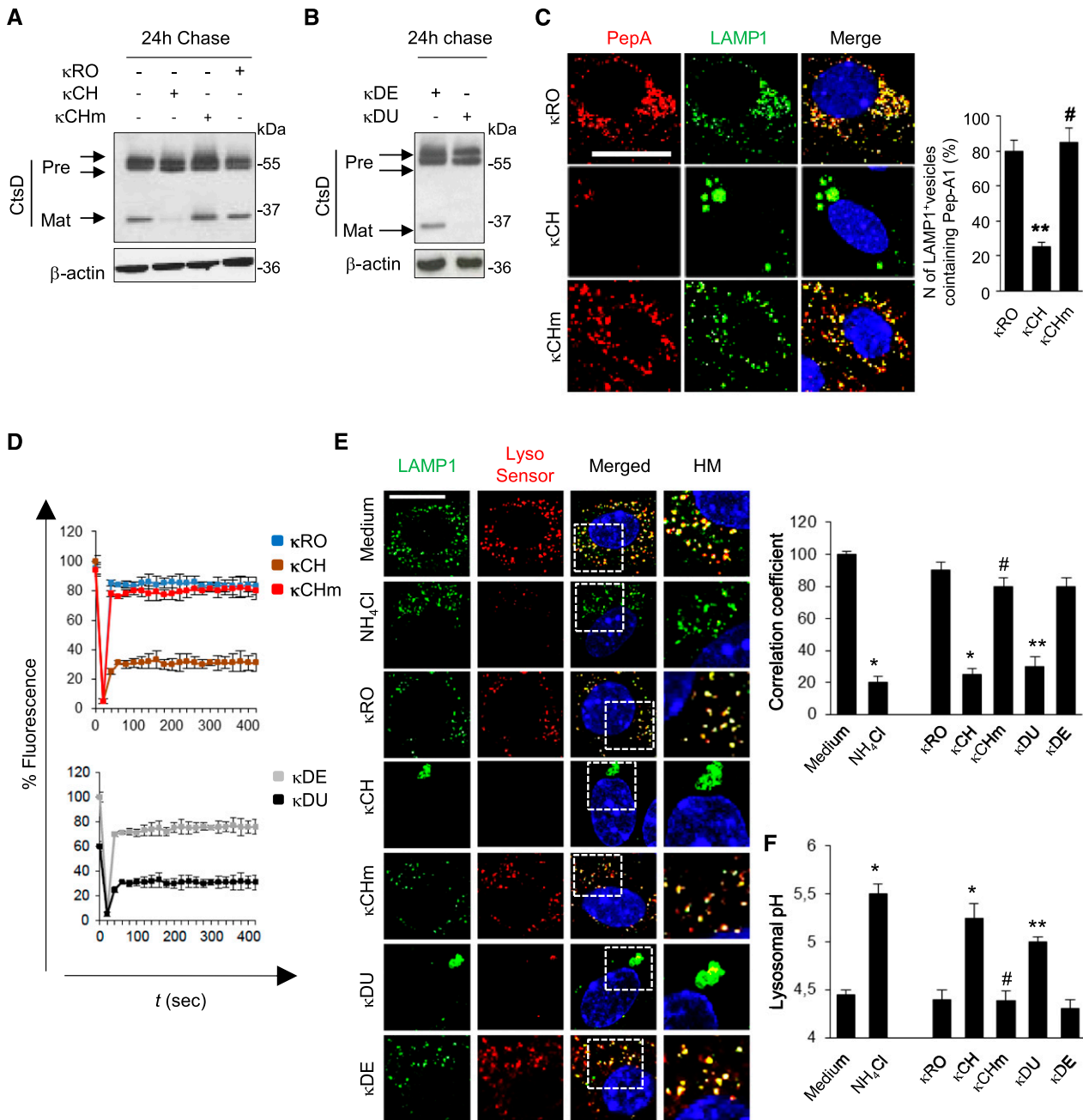


Figure 5. Defective proteolysis and acidification in lysosomes exposed to RFS-κLCs. Primary mPTCs were initially kept for 4 hours in serum-free medium, incubated with 25 μg/ml human κLCs for 1 hour at 4°C, and then, chased in κLCs-free culture medium for 24 hours at 37°C. (A and B) Representative immunoblots showing a reduced mature cathepsin-D (Mat; 32 kDa) in mPTCs exposed to the RFS-associated κCH or κDU versus control κRO, κCHm, or κDE; 20 μg total protein were loaded per lane. CtsD, cathepsin-D. (C) Cathepsin-D activity/trafficking assessed by confocal microscopy analysis of Bodipy-FL-PepA staining after exposure to κLCs. (C, right panel) Quantification of the Bodipy-positive dots. Scale bar, 10 μm. ***P*<0.01 κCH versus κRO (*n*=200 cells per condition); #*P*<0.01 κCHm versus κCH (*n*=200 cells per condition). (D) Measure of cathepsin-B activity in mPTCs exposed to κLCs for 24 hours followed by Magic Red fluorescence recovery (fluorescence recovery after photobleaching [FRAP]) microscopy analysis. FRAP data are displayed as percentages of recovery of prebleach fluorescence representative of ten recordings from different cells. (E) Effect of exposure of mPTCs to κLCs or NH₄Cl (20 nM for 6 hours) on LysoSensor DND-167 reactivity and colocalization with LAMP1. The LAMP1-positive compartments were LysoSensor positive in cells unexposed (medium alone) or exposed to κRO, κCHm, or κDE but LysoSensor negative in cells exposed to κCH or κDU, similar to NH₄Cl-treated cells. HM, high-magnification inset. Scale bar, 10 μm. (E, right panel) Quantification of LysoSensor DND-167/LAMP1 colocalization (correlation coefficient). **P*<0.003 versus unexposed cells or κRO (*n*=200 cells per condition); #*P*<0.01 κCHm versus κCH (*n*=200 cells per condition); ***P*<0.001 versus κDE (*n*=200 cells per condition). (F)

system, because colocalization between the endosomal markers Rab5 or Rab7 and LAMP1 outside the clusters was unaffected in these conditions (Supplemental Figure 4A). Also, the RFS- κ LCs did not interfere with the traffic from the trans-Golgi network to the endolysosomal compartment, which was evidenced by the lack of overlap between LAMP1 clusters and the cis-Golgi marker, GM130 (Supplemental Figure 4B). Changes in LAMP1 dynamics in mPTECs exposed to κ CH were not linked to alterations in Golgi structure or function, because LAMP1 clusters were still visible after Golgi disruption by Nocodazole and did not coaggregate with GM130-labeled Golgi fragments (Supplemental Figure 4B). Taken together, these results show that RFS- κ LCs specifically alter lysosome dynamics, with no effect on the endosomal and Golgi compartments.

Defective Proteolysis and Acidification in Lysosomes Exposed to RFS- κ LCs

To understand the mechanisms and consequences of aberrant lysosomal dynamics in PT cells exposed to RFS- κ LCs, we assessed the maturation of lysosomal hydrolases, such as cathepsin-B and -D. Relative to cells exposed to κ RO or κ CHm, a decreased proteolytic generation of the 32-kDa mature cathepsin-D was observed in cells exposed to κ CH or κ DU (Figure 5, A and B). The lysosomal cathepsin-D activity was tested, by incubating mPTECs with Bodipy-FL-Pepstatin A (PepA), a fluorescence-tagged PepA that binds to the active site of cathepsin-D in acidic lysosomes.²⁷ Although the majority of lysosomes were costained with PepA-labeled cathepsin-D in cells exposed to κ RO or κ CHm, the number of PepA-labeled vesicles and the colocalization of active cathepsin-D with LAMP1 were substantially lower in cells exposed to κ CH or κ DU (Figure 5C, Supplemental Figure 5).

The defective maturation of lysosomal hydrolases in mPTECs exposed to RFS- κ LCs was also confirmed by monitoring cathepsin-B activity *in situ* with Magic Red, a membrane-permeable substrate that fluoresces only after cleavage in acidic environment, followed by fluorescence recovery after photobleaching microscopy analysis. Whereas photobleaching of Magic Red-positive lysosomes was followed by a rapid ($\tau_{1/2}$ =18 seconds) and substantial (70%) recovery of the initial fluorescence in cells exposed to κ RO, κ CHm, or κ DE, the fluorescence recovery was slower and smaller in cells exposed to κ CH ($\tau_{1/2}$ =34 seconds; 25% recovery) or κ DU (Figure 5D).

To account for the impaired maturation of lysosomal cathepsins and lysosomal-mediated degradation, we assessed whether lysosomal acidification may be affected (Figure 5, E and F). We first incubated mPTECs with LysoSensor DND-167 to qualitatively measure lysosomal pH.²⁷ LysoSensor showed

strong fluorescence in virtually all LAMP1 vesicles of cells exposed to κ RO, κ CHm, and κ DE, whereas <20% of LAMP1 vesicles exhibited detectable fluorescence in cells exposed to κ CH or κ DU (Figure 5E). Measurement of lysosomal pH with quantitative ratiometric LysoSensor yellow/blue DND-160 revealed an increase of lysosomal pH in cells exposed to RFS- κ LCs from 4.5 ± 0.08 to 5.4 ± 0.01 , which was similar to that observed in PT cells treated with ammonium chloride (Figure 5E). These data indicate that RFS- κ LCs impair lysosomal acidification, causing a defect in hydrolase maturation and thus, altering the lysosomal degradative capacity.

Exposure to Selective RFS- κ LC Induces Cellular Proliferation and Defective Endocytosis

Finally, we tested whether the lysosomal alterations induced by κ LCs in mPTECs recapitulate the PT dysfunction/toxicity observed *in vivo*. Compared with control κ LCs (κ RO and κ CHm), exposure to the RFS-causing κ CH induced a major cell proliferation as assessed by bromodeoxyuridine incorporation (Figure 6A) and nuclear translocation of the proliferation markers PCNA and ZONAB (Figure 6, B and C). Dedifferentiation of the cells was evidenced by a decreased apical abundance of NaPi-IIa and megalin/cubilin (Figure 6, D and E, Supplemental Figure 6A), a marked decrease in albumin and transferrin uptake (Figure 6, F and G), and an increased retention of megalin and NaPi-IIa into EEA-1-positive endosomal compartment (Figure 6H). No noticeable changes in apoptosis markers were detected in mPTECs exposed to control or pathogenic κ LCs (Supplemental Figure 6B). No recovery in megalin expression and albumin endocytosis could be observed ≤ 72 hours after the incubation of mPTECs with κ CH versus κ CHm (Supplemental Figure 6, C and D).

These data show that the κ LCs associated with RFS induce a phenotype switch that is essentially similar to the PT changes observed *in vivo*.

DISCUSSION

This study sheds light on the molecular mechanisms causing renal PT dysfunction associated with monoclonal κ LCs. Using transgenic mice and primary cultures, we show that specific RFS- κ LCs accumulate in lysosomes, modify their dynamics and proteolytic function, and alter the reabsorptive capacity of the cells. These changes are similar to those observed in congenital lysosomal disorders causing RFS, including nephropathic cystinosis. Transgenic mice, which recapitulate the chronic production of monoclonal LCs in patients, and primary cultures of PT cells represent powerful tools to explore the toxicity triggered by individual LCs.

Lysosomal pH values were ratiometrically measured using LysoSensor yellow/blue DND-160. * $P < 0.01$ versus unexposed cells or κ RO ($n = 150$ cells per condition); # $P < 0.05$ versus κ CH ($n = 150$ cells per condition); ** $P < 0.01$ versus κ DE ($n = 150$ cells per condition). NH₄Cl, ammonium chloride.

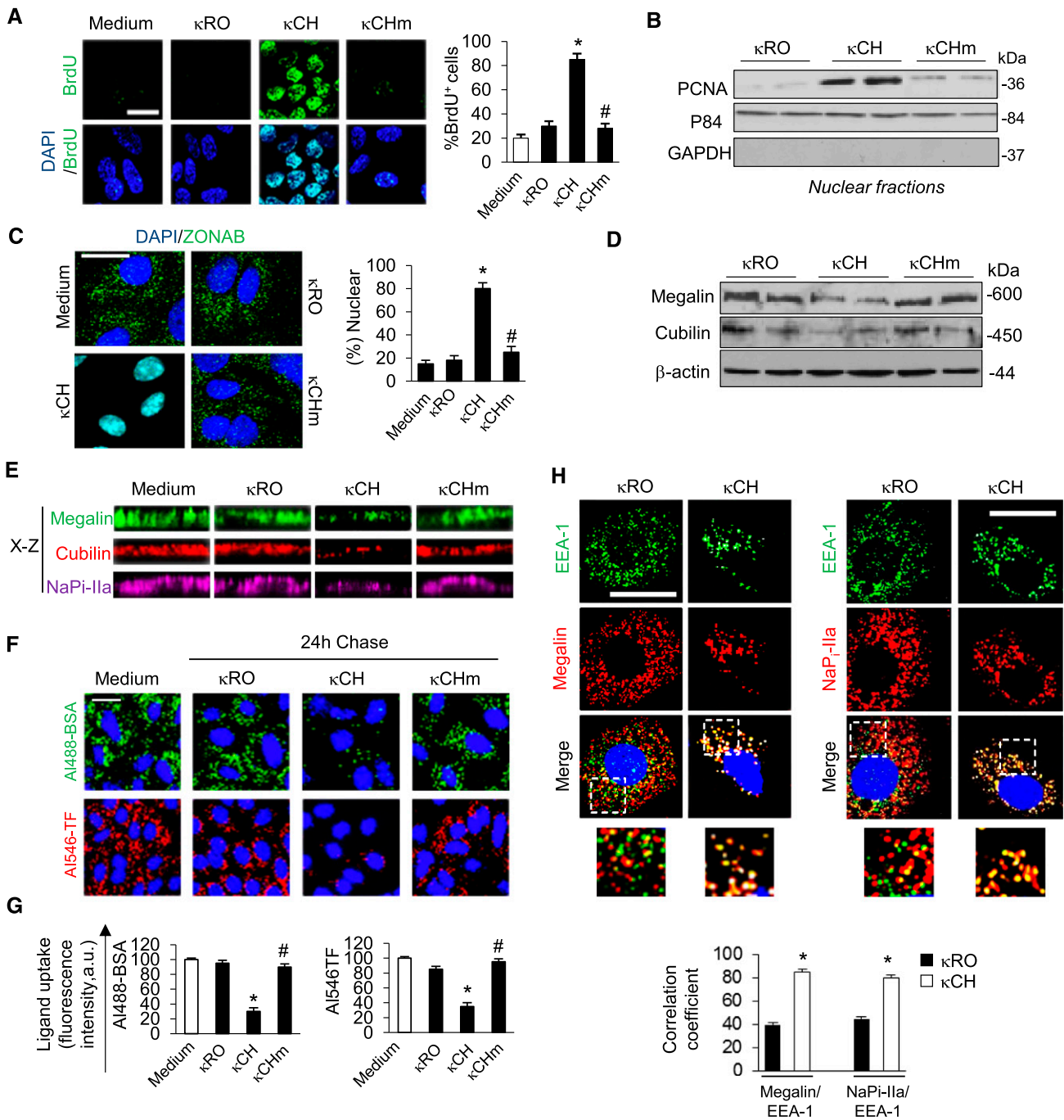


Figure 6. RFS-κLCs selectively induce proliferation, dedifferentiation, and defective endocytosis in mPTCs. Primary mPTCs were initially kept for 4 hours in serum-free medium, incubated with 25 μg/ml human κLCs for 60 minutes at 4°C, chased in κLCs-free culture medium for 24 hours at 37°C, and probed. (A) Bromodeoxyuridine (BrdU) staining and quantification. Nuclei were counterstained with DAPI (blue). Scale bar, 20 μm. **P*<0.05 versus unexposed or κRO cells (*n*=200 cells per condition); #*P*<0.01 versus κCH (*n*=200 cells per condition). (B) Representative immunoblots for PCNA in nuclear-enriched (p84-enriched, GAPDH-depleted) cell extracts. (C) Representative immunostaining for ZONAB, showing nuclear translocation in cells exposed to RFS-κCH compared with diffuse staining in cells exposed to κRO or κCHm. Nuclei were counterstained with DAPI (blue). Scale bar, 10 μm. (C, right panel) Quantification of ZONAB-positive nuclei. **P*<0.01 versus κRO (*n*=200 cells per condition); #*P*<0.01 versus κCH (*n*=200 cells per condition). (D) Representative immunoblots for megalin and cubilin in total cell lysates showing a decreased level of expression in cells exposed to κCH. (E) x-z Side view of a z stack showing decreased expression of megalin (green), cubilin (red), and NaPi-IIa (magenta) at the apical plasma membrane of mPTCs exposed to κCH versus κRO or κCHm. (F and G) Confocal microscopy and quantification of cell-associated uptake of Alexa Fluor-488(AI488)-bovine serum albumin (BSA) and Alexa Fluor-546-(AI546)-transferrin (TF). Nuclei were

Our investigations show a remarkable specificity of cellular damage induced by κ LCs. The changes in PT function observed in κ CH mice recapitulate the RFS of the corresponding patient, whereas no such changes were observed in κ DE mice expressing similar levels of κ LCs from a patient with AL amyloidosis but no RFS. Importantly, PT dysfunction was observed in the absence of renal failure and structural damage. These observations were extended *in vitro*: exposure of mPTCs to low concentrations of RFS- κ LCs (κ CH or κ DU) induced marked changes in lysosomal function and cellular phenotype, which were not observed with control κ LCs. Interestingly, the V domain in κ CH mice is derived from the *V κ 1-33* gene, which is frequently associated with RFS in human,²⁸ showing that subtle changes in the V sequences are required to induce RFS. Likewise, a single mutation in the CDR1 of the κ CH (Ala to Ser; κ CHm), precluding the intracellular crystal formation in PT cells without affecting protease resistance of the V domain,¹⁹ strongly decreased the toxicity of the corresponding κ LCs in mPTCs. Because no crystals were detected in lysosomes of mPTCs exposed to RFS- κ LCs, probably reflecting the duration of experiments and low concentrations of κ LCs used *in vitro*, these results suggest that neither *in vitro* protease resistance of the V domain nor crystal formation account for the toxicity of RFS- κ LC. Conversely, subtle changes in V sequences can have tremendous consequences for renal toxicity.

Although monoclonal LC-associated PT dysfunction is a frequent cause of RFS in adults, the molecular mechanisms involved remain debated. Previous studies showed that free LCs can block metabolites transport and promote oxidative stress, leading to NF- κ B activation and inflammation.³ However, characteristics of cellular and animal models cause significant limitations to investigation of mechanisms of PT dysfunction in general and potential defects in the endolysosomal apparatus in particular.²⁰ Immortalized cell systems may be dedifferentiated, with loss of polarity and low levels (if any) of endogenous receptors and endocytic uptake, which is problematic for studies of endolysosomal disorders in PT cells.^{3,5} *In vivo*, PT cell dysfunction was observed after injection of high quantities of LCs (1 mg/ml or more) in rat or mouse,^{16,29} a condition that does not reflect the chronic delivery of low doses of LCs during smoldering myeloma or MGUS, which typically underlies hematologic disorders associated with RFS.⁹ The use of transgenic mice models producing human monoclonal LCs and differentiated primary cultures of PT cells is, thus, particularly useful to investigate mechanisms of epithelial differentiation in response to monoclonal LCs.

We show that RFS- κ LCs alter cell dynamics and lysosome functions *in vivo* and *in vitro*. These changes are caused by

accumulation of RFS-causing κ LCs in enlarged, perinuclear lysosomes. The lysosomal defect is evidenced by morphologic abnormalities and defective processing/degradation of LCs likely resulting from the defective maturation and activity of cathepsin-B and -D revealed by fluorescence recovery after photobleaching analysis and PepA staining, respectively. Importantly, these changes in lysosome function occur with no evidence for crystals *in vitro* and in absence of apoptosis. Furthermore, RFS- κ LCs induce a defect in vesicular acidification as monitored by LysoSensor imaging and lysosomal pH. The conjugation of impaired lysosomal dynamics, defective hydrolyase maturation, and altered lysosomal degradative capacity is strikingly similar to the changes observed in nephropathic cystinosis, a congenital disorder caused by inactivating mutations in the lysosomal transporter cystinosin.¹³ Loss of cystinosin function results in the accumulation of cystine inside lysosomes, invariably causing RFS.³⁰ Thus, lysosomal accumulation of specific κ LCs or cystine may have the same functional consequences in PT cells.

Several mechanisms could sustain the lysosomal toxicity of RFS- κ LCs. After reabsorbed and trafficked to lysosomes, the κ LCs may bind to and inactivate cathepsins or other proteases or produce a form that is resistant to lysosomal hydrolysis. In turn, the prolonged retention of such κ LCs within lysosomes may further impair the processing of acid hydrolases, promoting additional cargo accumulation. As suggested by our results, RFS- κ LCs also impair lysosomal acidification, which may result from an effect on V-ATPase activity caused by sequestration or defective trafficking of V-ATPase subunits or changes in lysosomal membrane cholesterol levels.³¹ Detailed temporal analyses of the lipid metabolism and pH changes could help to answer some of these questions.

Other than the lysosomal defect, RFS- κ LCs also cause alterations in receptor-mediated endocytosis, with defective expression of megalin and cubilin. These alterations, observed in cells accumulating RFS- κ LCs, account for the loss of LMW ligands in urine. In absence of transcriptional defects, the loss of apical receptors is similar to that observed in the mouse and cellular models of Dent disease.¹² Defects in receptor-mediated endocytosis are also directly involved in nephropathic cystinosis¹³ and a constitutive KO of the α 4-subunit of the V-ATPase, also causing lysosomal protein accumulation.³² We also show that a second apical pathway operating in PT cells is defective in LC-associated RFS: the κ CH mice show phosphaturia and decreased expression of the phosphate cotransporter NaPi-IIa. Likewise, NaPi-IIa is only decreased in cells exposed to the toxic κ CH and κ DU. Because phosphate reabsorption by NaPi-IIa is under the control of the

counterstained with DAPI (blue). * $P < 0.01$ versus unexposed or κ RO cells ($n = 150$ cells per condition); # $P < 0.05$ versus κ CH ($n = 150$ cells per condition). (H) Double immunofluorescence staining for EEA-1 (green)/megalin (red) or EEA-1 (green)/NaPi-IIa (red) in mPTCs exposed to κ LCs for 24 hours. Nuclei were counterstained with DAPI (blue). Dotted white squares contain high magnification images. Scale bar, 10 μ m. (H, lower panel) Quantitative measurement of EEA-1/megalin or EEA-1/NaPi-IIa colocalizations (correlation coefficient). * $P < 0.01$ κ CH versus κ RO. DAPI, 4', 6'-diamidino-2-phenylindole, EEA-1, early endosome antigen-1.

parathyroid hormone through its apical and basal receptors, one can hypothesize that a trafficking defect similar to that observed in *Ctns*^{-/-} and *Cln5*^{-/-} kidneys may be involved.^{12,13}

In addition to defective apical transport, abnormal proliferation is often observed in diseased PT cells.^{13,24,33} Increased proliferation was consistently observed in κ CH kidneys and mPTCs exposed to RFS- κ LCs as indicated by the PCNA and cyclin-D1 markers and bromodeoxyuridine incorporation. Our data suggest the involvement of the Y-box transcription factor ZONAB, which is active during nephrogenesis and PT maturation. When epithelial cells are confluent and express differentiated tight junctions, ZONAB is retained by the cytosolic SH3 domain of ZO-1,³⁴ preventing its nuclear translocation and activation of target genes, including PCNA and cyclin-D1. On exposure to RFS- κ CH but not to control κ LCs, we observed a nuclear translocation of ZONAB associated with markers of proliferation. Previous studies have shown that a delicate balance between factors involved in proliferation and others involved in differentiation operates in PT cells.²⁴ The balance can be defective, for instance, in cystinosis, where increased proliferation and dedifferentiation of PT cells are associated with abnormal activity of ZONAB caused by defective intercellular junctions.¹³ This study does not provide a direct correlation between increased rate of proliferation and dedifferentiation of PT cells. The potential link between the two events could be elucidated by intervention studies targeting the early events induced by the pathogenic κ LCs.

Could these changes reflect an adaptation to the uptake of toxic κ LCs? mPTCs exposed to high concentrations of albumin decrease the expression of megalin.³⁵ By analogy, PT cells could, thus, inhibit endocytosis and accumulation of LCs in case of monoclonal gammopathies.³⁶ A potential mechanism, suggested by the increased association of megalin with EEA-1-positive endosomes, may be retention into the endolysosomal compartment, with prolonged activation of the EGF receptor causing cell dedifferentiation.³⁷ Would that mean a potential reversibility of the changes observed in PT cells exposed to toxic κ LCs? *In vivo* studies showed the persistence of tubular crystal inclusions in the κ CH mice \leq 2 months after the conditional deletion of the κ LCs.²¹ Furthermore, we could not observe a recovery in endocytosis and receptor expression \leq 72 hours after the incubation of mPTCs with κ CH. Future studies should test whether promoting the clearance of lysosomal storage, involving LYSO-phagy and/or specific transcription factors, such as MiT/TFEB, would improve the differentiation of PT cells.^{38,39}

In conclusion, our studies show that RFS- κ LCs induce profound alterations in cell dynamics and lysosome function, sustaining a loss of apical transport capacity. These data provide a basis for the differential LCs toxicity in the kidney tubule before the onset of renal failure. Insights into these early events may provide new targets to alleviate the burden caused by the urinary loss of vital metabolites in monoclonal gammopathies.

CONCISE METHODS

Detailed methods used for mouse models, renal function parameters, histologic analysis, electron microscopy and immunogold analyses, production of human κ LCs *in vitro*, isolation and primary cultures of mPTCs, quantification of LC uptake, quantitative real-time PCR, subcellular fractionation, immunoblotting, immunofluorescence and confocal microscopy, quantification of lysosome distribution, lysosomal pH measurement, and statistical analyses as well as antibodies, reagents, and primers are provided in Supplemental Material.

ACKNOWLEDGMENTS

The authors acknowledge I. Bouteau, P.J. Courtoy, A. Kaech, E. Olinger, C. Pierreux, C. Raggi, and G. Touchard for discussions and/or preliminary experiments; C.A. Wagner, P.J. Verroust, and R. Kozyraki for reagents; B. Fernandez and N. Quellard for electron microscopy assistance; and F. Di Meo for three-dimensional modelling. Imaging was performed with equipment maintained by the Center for Microscopy and Image Analysis, University of Zurich.

A.B. is funded by French Government fellowships. This work was supported by the Fonds National de la Recherche Scientifique and the Fonds de la Recherche Scientifique Médicale (to O.D.), European Community's Seventh Framework Programme FP7/2007-2013 Grant 305608 (EURenOmics) (to O.D.), the Cystinosis Research Foundation Grant CRFS-2014-005 (to O.D. and A.L.), Swiss National Science Foundation Project Grant 310030-146490 (to O.D.), the Clinical Research Priority Program Molecular Imaging Network Zurich of the University of Zurich, the Conseil Régional du Limousin, and the French National Reference Center for Amyloid-Light Chain (AL) Amyloidosis (SL220100601332 to C.S and A.B.).

DISCLOSURES

None.

REFERENCES

- Kyle RA, Therneau TM, Rajkumar SV, Larson DR, Plevak MF, Offord JR, Dispenzieri A, Katzmann JA, Melton LJ 3rd: Prevalence of monoclonal gammopathy of undetermined significance. *N Engl J Med* 354: 1362–1369, 2006
- Leung N, Bridoux F, Hutchison CA, Nasr SH, Cockwell P, Ferman J-P, Dispenzieri A, Song KW, Kyle RA; International Kidney and Monoclonal Gammopathy Research Group: Monoclonal gammopathy of renal significance: When MGUS is no longer undetermined or insignificant. *Blood* 120: 4292–4295, 2012
- Sanders PW: Mechanisms of light chain injury along the tubular nephron. *J Am Soc Nephrol* 23: 1777–1781, 2012
- Christensen EI, Birn H, Storm T, Weyer K, Nielsen R: Endocytic receptors in the renal proximal tubule. *Physiology (Bethesda)* 27: 223–236, 2012
- Batuman V, Verroust PJ, Navar GL, Kaysen JH, Goda FO, Campbell WC, Simon E, Pontillon F, Lyles M, Bruno J, Hammond TG: Myeloma light chains are ligands for cubilin (gp280). *Am J Physiol* 275: F246–F254, 1998

6. Hutchison CA, Batuman V, Behrens J, Bridoux F, Sirac C, Dispenzieri A, Herrera GA, Lachmann H, Sanders PW; International Kidney and Monoclonal Gammopathy Research Group: The pathogenesis and diagnosis of acute kidney injury in multiple myeloma. *Nat Rev Nephrol* 8: 43–51, 2012
7. Ying W-Z, Wang P-X, Aaron KJ, Basnayake K, Sanders PW: Immunoglobulin light chains activate nuclear factor- κ B in renal epithelial cells through a Src-dependent mechanism. *Blood* 117: 1301–1307, 2011
8. Maldonado JE, Velosa JA, Kyle RA, Wagoner RD, Holley KE, Salassa RM: Fanconi syndrome in adults. A manifestation of a latent form of myeloma. *Am J Med* 58: 354–364, 1975
9. Messiaen T, Deret S, Mougnot B, Bridoux F, Dequiedt P, Dion JJ, Makdassi R, Meeus F, Pourrat J, Touchard G, Vanhille P, Zaoui P, Aucouturier P, Ronco PM: Adult Fanconi syndrome secondary to light chain gammopathy. Clinicopathologic heterogeneity and unusual features in 11 patients. *Medicine (Baltimore)* 79: 135–154, 2000
10. Sirac C, Bridoux F, Essig M, Devuyt O, Touchard G, Cogné M: Toward understanding renal Fanconi syndrome: Step by step advances through experimental models. *Contrib Nephrol* 169: 247–261, 2011
11. Igarashi T: Fanconi syndrome. In: *Pediatric Nephrology*, 6th Ed., edited by Avner E, Harmon W, Niaudet P, Yoshikawa N, Berlin, Springer-Verlag, 2009, pp 1039–1067
12. Christensen EI, Devuyt O, Dom G, Nielsen R, Van der Smissen P, Verroust P, Leruth M, Guggino WB, Courtoy PJ: Loss of chloride channel CLC-5 impairs endocytosis by defective trafficking of megalin and cubilin in kidney proximal tubules. *Proc Natl Acad Sci U S A* 100: 8472–8477, 2003
13. Raggi C, Luciani A, Nevo N, Antignac C, Terryn S, Devuyt O: De-differentiation and aberrations of the endolysosomal compartment characterize the early stage of nephropathic cystinosis. *Hum Mol Genet* 23: 2266–2278, 2014
14. Herrera GA: Proximal tubulopathies associated with monoclonal light chains: The spectrum of clinicopathologic manifestations and molecular pathogenesis. *Arch Pathol Lab Med* 138: 1365–1380, 2014
15. Sanders PW, Herrera GA, Galla JH: Human Bence Jones protein toxicity in rat proximal tubule epithelium in vivo. *Kidney Int* 32: 851–861, 1987
16. Sanders PW, Herrera GA, Chen A, Booker BB, Galla JH: Differential nephrotoxicity of low molecular weight proteins including Bence Jones proteins in the perfused rat nephron in vivo. *J Clin Invest* 82: 2086–2096, 1988
17. Pote A, Zwizinski C, Simon EE, Meleg-Smith S, Batuman V: Cytotoxicity of myeloma light chains in cultured human kidney proximal tubule cells. *Am J Kidney Dis* 36: 735–744, 2000
18. Aucouturier P, Bauwens M, Khamlichi AA, Denoroy L, Spinelli S, Touchard G, Preud'homme JL, Cogné M: Monoclonal Ig L chain and L chain V domain fragment crystallization in myeloma-associated Fanconi's syndrome. *J Immunol* 150: 3561–3568, 1993
19. Decourt C, Rocca A, Bridoux F, Vrtovnik F, Preud'homme JL, Cogné M, Touchard G: Mutational analysis in murine models for myeloma-associated Fanconi's syndrome or cast myeloma nephropathy. *Blood* 94: 3559–3566, 1999
20. Dickson LE, Wagner MC, Sandoval RM, Molitoris BA: The proximal tubule and albuminuria: Really! *J Am Soc Nephrol* 25: 443–453, 2014
21. Sirac C, Bridoux F, Carrion C, Devuyt O, Fernandez B, Goujon J-M, El Hamel C, Aldigier J-C, Touchard G, Cogné M: Role of the monoclonal kappa chain V domain and reversibility of renal damage in a transgenic model of acquired Fanconi syndrome. *Blood* 108: 536–543, 2006
22. Terryn S, Jouret F, Vandenabeele F, Smolders I, Moreels M, Devuyt O, Steels P, Van Kerkhove E: A primary culture of mouse proximal tubular cells, established on collagen-coated membranes. *Am J Physiol Renal Physiol* 293: F476–F485, 2007
23. Reed AAC, Loh NY, Terryn S, Lippiat JD, Partridge C, Galvanovskis J, Williams SE, Jouret F, Wu FTF, Courtoy PJ, Nesbit MA, Rorsman P, Devuyt O, Ashcroft FM, Thakker RV: CLC-5 and KIF3B interact to facilitate CLC-5 plasma membrane expression, endocytosis, and microtubular transport: Relevance to pathophysiology of Dent's disease. *Am J Physiol Renal Physiol* 298: F365–F380, 2010
24. Gailly P, Jouret F, Martin D, Debaix H, Parreira KS, Nishita T, Blanchard A, Antignac C, Willnow TE, Courtoy PJ, Scheinman SJ, Christensen EI, Devuyt O: A novel renal carbonic anhydrase type III plays a role in proximal tubule dysfunction. *Kidney Int* 74: 52–61, 2008
25. Leboulleux M, Lelong B, Mougnot B, Touchard G, Makdassi R, Rocca A, Noel LH, Ronco PM, Aucouturier P: Protease resistance and binding of Ig light chains in myeloma-associated tubulopathies. *Kidney Int* 48: 72–79, 1995
26. Nath KA: Receptor-mediated endocytosis is a Trojan horse in light-chain nephrotoxicity. *J Am Soc Nephrol* 21: 1065–1066, 2010
27. Lee J-H, Yu WH, Kumar A, Lee S, Mohan PS, Peterhoff CM, Wolfe DM, Martinez-Vicente M, Massey AC, Sovak G, Uchiyama Y, Westaway D, Cuervo AM, Nixon RA: Lysosomal proteolysis and autophagy require presenilin 1 and are disrupted by Alzheimer-related PS1 mutations. *Cell* 141: 1146–1158, 2010
28. Déret S, Denoroy L, Lamarine M, Vidal R, Mougnot B, Frangione B, Stevens FJ, Ronco PM, Aucouturier P: Kappa light chain-associated Fanconi's syndrome: Molecular analysis of monoclonal immunoglobulin light chains from patients with and without intracellular crystals. *Protein Eng* 12: 363–369, 1999
29. Khan A-M, Li M, Balamuthusamy S, Maderdrut JL, Simon EE, Batuman V: Myeloma light chain-induced renal injury in mice. *Nephron, Exp Nephrol* 116: e32–e41, 2010
30. Gahl WA, Thoene JG, Schneider JA: Cystinosis. *N Engl J Med* 347: 111–121, 2002
31. Cox BE, Griffin EE, Ullery JC, Jerome WG: Effects of cellular cholesterol loading on macrophage foam cell lysosome acidification. *J Lipid Res* 48: 1012–1021, 2007
32. Hennings JC, Picard N, Huebner AK, Stauber T, Maier H, Brown D, Jentsch TJ, Vargas-Poussou R, Eladari D, Hübner CA: A mouse model for distal renal tubular acidosis reveals a previously unrecognized role of the V-ATPase a4 subunit in the proximal tubule. *EMBO Mol Med* 4: 1057–1071, 2012
33. Lima WR, Parreira KS, Devuyt O, Caplanusi A, N'kuli F, Marien B, Van Der Smissen P, Alves PMS, Verroust P, Christensen EI, Terzi F, Matter K, Balda MS, Pierreux CE, Courtoy PJ: ZONAB promotes proliferation and represses differentiation of proximal tubule epithelial cells. *J Am Soc Nephrol* 21: 478–488, 2010
34. Balda MS, Matter K: Tight junctions and the regulation of gene expression. *Biochim Biophys Acta* 1788: 761–767, 2009
35. Caruso-Neves C, Pinheiro AAS, Cai H, Souza-Menezes J, Guggino WB: PKB and megalin determine the survival or death of renal proximal tubule cells. *Proc Natl Acad Sci U S A* 103: 18810–18815, 2006
36. Basnayake K, Ying W-Z, Wang P-X, Sanders PW: Immunoglobulin light chains activate tubular epithelial cells through redox signaling. *J Am Soc Nephrol* 21: 1165–1173, 2010
37. Hallman MA, Zhuang S, Schnellmann RG: Regulation of de-differentiation and redifferentiation in renal proximal tubular cells by the epidermal growth factor receptor. *J Pharmacol Exp Ther* 325: 520–528, 2008
38. Maejima I, Takahashi A, Omori H, Kimura T, Takabatake Y, Saitoh T, Yamamoto A, Hamasaki M, Noda T, Isaka Y, Yoshimori T: Autophagy sequesters damaged lysosomes to control lysosomal biogenesis and kidney injury. *EMBO J* 32: 2336–2347, 2013
39. Martina JA, Diab HI, Li H, Puertollano R: Novel roles for the MiTF/TFE family of transcription factors in organelle biogenesis, nutrient sensing, and energy homeostasis. *Cell Mol Life Sci* 71: 2483–2497, 2014

This article contains supplemental material online at <http://jasn.asnjournals.org/lookup/suppl/doi:10.1681/ASN.2015050581/-/DCSupplemental>.